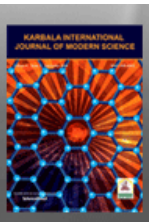
Karbala International Journal of Modern Science

Manuscript 3375

Removal of selenium ions from contaminated aqueous solutions by adsorption using lemon peels as a non-conventional medium

Alanood A. Alsarayreh

Suha Anwer Ibrahim

Salem Jawad Alhamd

Thekra Atta Ibrahim

Mohammed Nsaif Abbas

Removal of selenium ions from contaminated aqueous solutions by adsorption using lemon peels as a non-conventional medium

Abstract

The disposal of heavy metals from various activities has become a pervasive issue. The investigation of sustain-able, low-cost adsorbents for the remediation of these hazardous pollutants has been widely disregarded. This research emphasizes the recovery of selenium ions from contaminated water using lemon peels as a cost-effective adsorbent. The adsorption was explored in a batch unit under various operational parameters, including initial selenium concentration (1-90 ppm), pH (1-11), agitation speed (100-500 rpm), adsorbent dose (0.4-5.5 g), contact time (5-180 minutes), and temperature (25-55 °C). The BET surface area of the lemon peels was found to be 27.86 m^2/g before adsorption and 2.18 m^2/g after adsorption. FTIR analysis exposed the disappearance or shifting of several peaks, while the FESEM analysis showed significant changes in the surface morphology of the lemon peels due to its interaction with selenium. The results indicated that lemon peels are highly effective at removing selenium, attaining an efficiency of over 87% under optimal conditions: pH 8, agitation speed of 450 rpm, initial selenium concentration of 86 ppm, adsorbent dose of 5 g, contact time of 150 minutes, and temperature of 25 °C. The experimental results were analyzed using isothermal, kinetic, and thermodynamic methodologies. The mathematical model confirmed that the Langmuir theory is the most effective at representing the adsorption isotherm, while in terms of kinetic, the adsorption followed the inter-particle diffusion model, as indicated by the correlation coefficient (R^2) values. Moreover, the adsorption process was found to be spontaneous, exothermic, and associated with low entropy over the studied temperature range.

Keywords

Adsorption, aqueous solution, lemon peels, selenium, zero residual level (ZRL)

RESEARCH PAPER

Removal of Selenium Ions From Contaminated Aqueous Solutions by Adsorption Using Lemon Peels as a Non-conventional Medium

Alanood A. Alsarayreh [a], Suha A. Ibrahim [b], Salem J. Alhamd [c], Thekra A. Ibrahim [d], Mohammed N. Abbas [e,*]

[a] Chemical Engineering Department, Faculty of Engineering, Mutah University, Al Karak, Jordan
[b] Environmental Engineering Department, College of Engineering, Mustansiriyah University, Baghdad, Iraq
[c] Department of Petroleum Engineering, College of Engineering, University of Kerbala, Kerbala, Iraq
[d] Department of Biology, College of Education for Pure Science, University of Diyala, Diyala, Iraq
[e] Materials Engineering Department, College of Engineering, Mustansiriyah University, Baghdad, Iraq

Abstract

The disposal of heavy metals from various activities has become a pervasive issue. The investigation of sustain-able, low-cost adsorbents for the remediation of these hazardous pollutants has been widely disregarded. This research emphasizes the recovery of selenium ions from contaminated water using lemon peels as a cost-effective adsorbent. The adsorption was explored in a batch unit under various operational parameters, including initial selenium concentration (1−90 ppm), pH (1−11), agitation speed (100−500 rpm), adsorbent dose (0.4−5.5 g), contact time (5−180 min), and temperature (25−55 °C). The BET surface area of the lemon peels was found to be 27.86 m^2/g before adsorption and 2.18 m^2/g after adsorption. FTIR analysis exposed the disappearance or shifting of several peaks, while the FESEM analysis showed significant changes in the surface morphology of the lemon peels due to its interaction with selenium. The results indicated that lemon peels are highly effective at removing selenium, attaining an efficiency of over 87% under optimal conditions: pH 8, agitation speed of 450 rpm, initial selenium concentration of 86 ppm, adsorbent dose of 5 g, contact time of 150 min, and temperature of 25 °C. The experimental results were analyzed using isothermal, kinetic, and thermodynamic methodologies. The mathematical model confirmed that the Langmuir theory is the most effective at representing the adsorption isotherm, while in terms of kinetic, the adsorption followed the inter-particle diffusion model, as indicated by the correlation coefficient (R^2) values. Moreover, the adsorption process was found to be spontaneous, exothermic, and associated with low entropy over the studied temperature range.

Keywords: Adsorption, Aqueous solution, Lemon peels, Selenium, Zero residual level (ZRL)

1. Introduction

Heavy metals are a group of metals characterized by their large atomic weight and high density, typically having densities at least five times greater than that of water [1]. These metals exhibit toxic properties even at low concentrations, posing significant risks to both health and the environment [2]. The term "heavy metals" refers to the physical characteristics of these metals, specifically their large atomic weights and high densities, which distinguish them from other metals [3]. These properties cause them to accumulate in biological environments, enhancing their toxic effects on living organisms [4]. Heavy metals can be divided into two categories. The first includes the elements that are harmful to humans and cause chronic diseases and cancers, such as mercury (Hg), arsenic (As), barium (Ba), cadmium (Cd), chromium (Cr), cobalt (Co), lead (Pb), lithium (Li), manganese (Mn), molybdenum

Received 25 June 2024; revised 29 September 2024; accepted 1 October 2024.
Available online 25 October 2024

* Corresponding author.
E-mail address: mohammed.nsaif.abbas@uomustansiriyah.edu.iq (M.N. Abbas).

https://doi.org/10.33640/2405-609X.3375

(Mo), nickel (Ni), thallium (Tl), tin (Sn) vanadium (V), and others [5]. The second category consists of the heavy metals that humans need in limited quantities, but if they exceed the specified values, they lead to various health damages. Some of these elements, are iron (Fe), zinc (Zn), copper (Cu), selenium (Si) … etc. [6]. Industrially, the metals in the latter category, especially selenium, are used in wide range of different applications like semiconductors, optical devices, in the glass industry to reduce darkness, in some types of batteries, as well as in nutritional supplements due to its important biological importance, and also due to its harmful effects in the event of accumulation and taking excessive doses [7]. Selenium is an essential trace element that is crucial for human health in small quantities. It plays a vital role in the functioning of antioxidant enzymes, protecting cells from oxidative damage. Additionally, selenium supports the immune system and the thyroid gland's proper functioning [8]. Although selenium is essential in small amounts, excessive exposure can cause toxicity known as selenosis, which includes symptoms such as hair loss, nail damage, skin irritation, nervous system problems, and digestive disorders [9]. The World Health Organization (WHO) recommends that the maximum permissible concentration of selenium in drinking water is 0.04 mg/L [10]. In the United States, the Environmental Protection Agency (EPA) sets the maximum permissible limit at 0.05 ppm (EPA, 2022), while according to "The Iraqi quality specification," selenium is contaminated when it exceeds 0.1 mg/L [10,11]. Thus, it is essential to monitor the levels of heavy metals, especially selenium, in drinking water, wastewater, and other aqueous solutions. This is particularly important in regions where activities involving these metals occur [12]. There are numerous methods and technologies employed for treating polluted water, especially in the removal of heavy metals. These include precipitation, reverse osmosis, ion exchange, advanced oxidation processes, biological methods, evaporation, reduction, adsorption, ultrafiltration, and others [13]. Each of these methods has demonstrated effectiveness in treating pollutants, but they all have certain limitations. These include high costs, the need for large areas and specialized equipment, requirements for pre-treatment, high energy consumption, and the accumulation of toxic waste post-process, among others [14]. Adsorption technology has been recognizing as a cost-effective method for treatment in comparison to other methods. It does not require specialized equipment or extensive space, and it is versatile enough to treat various pollutants at different concentrations [15]. Activated carbon is widely recognized as one of the most renowned and effective adsorption media. It possesses the capability to address numerous pollutants owing to its distinctive properties, such as a high surface area and a chemical composition rich in active sites [16]. Nevertheless, the high manufacturing costs and 10–15% weight loss during each regeneration process have driven specialists to seek out efficient and cost-effective alternatives [17]. Among the alternatives that have proven successful are industrial and agricultural waste such as aluminum foil [18], banana peels [19], orange peels [20], mandarin peels [21], rice husks [22], watermelon rinds [23], lemon peels [24], waste tea leaves [25], egg shells [26], algae [27], water hyacinth [28], sunflower seed hulls [29], buckthorn leaves [30], Eucalyptus leaves [31], and others. These adsorbents have succeeded in being a successful alternative to activated carbon, and have proven their efficiency when it comes removing various types of pollutants such as heavy metals [32], dyes [33], organic acids [34], organic toxins [35], pesticides [36], drugs [37], biological stains [5], radioactive elements [38], oil residues [39], and hardness of water [40] from water, crude oil [41], and soil [42]. Despite these

Nomenclature

b	Adsorption heat constant ($J \cdot mol^{-1}$)
C_e	Equilibrium concentration of adsorbent (ppm)
C_i	Initial concentrations of adsorbent (ppm)
C_f	Final concentrations of adsorbent (ppm)
I	Constant of intra-particle diffusion model ($g \cdot mg^{-1}$)
K_F	Freundlich constant [$(mg \cdot g^{-1}).(l \cdot mg^{-1})^{1/n}$]
K_L	Constant of Langmuir isotherm model ($l \cdot mg^{-1}$)
K_T	Temkin constant ($l \cdot g^{-1}$)
k_1	1st order rate constant (min^{-1})
k_2	2nd order rate constant ($g \cdot mg^{-1} \cdot min^{-1}$)
k_{ad}	Adsorption equilibrium coefficient (–)
k_P	Intra-particle diffusion rate constant ($g \cdot mg^{-1} \cdot min^{-0.5}$)
m	Mass of adsorbent media (g)
n	Adsorption intensity of Freundlich isotherm model (–)
q_e	Capacity of adsorption at equilibrium ($mg \cdot g^{-1}$)
q_{max}	Maximum capacity of adsorption ($mg \cdot g^{-1}$)
q	Capacity of adsorption at any time ($mg \cdot g^{-1}$)
$\%R$	is the percentage removal (–)
$\mathbb{R}$	Universal gas constant (8.3144 $J \cdot mol^{-1} \cdot K^{-1}$)
T	Absolute temperature (K)
t	Time of adsorption (min)
V	Volume of solution (l)
α	Initial rate of adsorption ($mg \cdot g^{-1} \cdot min^{-1}$)
β	Desorption constant ($g \cdot mg^{-1}$)
ΔH	Enthalpy change ($J \cdot mol^{-1}$)
ΔS	Entropy change ($J \cdot mol^{-1} \cdot K^{-1}$)
ΔG	Gibbs free energy ($kJ \cdot mol^{-1}$)

advantages, the accumulation of toxic residues is the only remaining obstacle to developing adsorption technology using industrial or agricultural waste [5]. This obstacle was solved through the concept of Zero Residue Level (ZRL), through which it was possible to convert these residues into useful materials and utilize them in different ways. They can be converted into a raw material for producing chemical materials such as acetone [43], bioethanol [44], a soil fertilizer [45], or a rodenticide due to its toxic effects on mice [46] and rabbits [47], or as a radiation absorbent material in medical radiology rooms [48]. It can also be a reinforcement material for concrete [49], used in the preparation of nanomaterials [50], or used as a catalyst [51] etc. Lemon peels are one of the agricultural wastes materials resulting from the consumption of lemon fruit. They are produced in large quantities, as each lemon wastes between 5 and 15% of its weight as peel. According to 2022 estimates, the global production of lemon was more than 21.5 million tons in 2023–24, and is forecast up 225,000, i.e. the amount of waste peels is estimated to be more than 5.5 million tons, representing a very large mass that can be used in an environmentally-friendly way instead of throwing it into landfills as waste [52]. Lemon peels contain many vital components such as fiber, vitamins, minerals, and plant compounds such as flavonoids and essential oils (limonene), so they are considered non-toxic and low-cost materials [53]. At the same time, they have multiple functional groups and a suitable surface area, which makes them a target for researchers looking for suitable alternatives to well-known adsorption media such as activated carbon, alumina, zeolite, and silica, and unconventional adsorption materials that can be easily used to purify aqueous solutions and recover various pollutants, including heavy metals [54]. This study aims to explore the potential of lemon peels, an abundant and low-value agricultural waste, as an adsorbent for removing selenium from contaminated water. Utilizing a batch-type adsorption unit, various operating conditions were tested to evaluate the isothermal, kinetic, and thermodynamic behaviors of the adsorption process.

2. Materials and methods

2.1. Adsorbent media preparation (lemon peels)

The lemon peels utilized in this research were sourced from household consumption. These peels, known for their yellow color and sour taste, constitute approximately 7–13% of the total weight of the lemon fruit. The BET analysis determined that the peels had a surface area of 27.86 m^2/g. The peels were transported to the laboratory at a rate of three batches per week. Each batch of peels was immediately washed with excess tap water for at least three times to get rid of any dirt, dust and any other residues attached to it. Then they were washed with distilled water twice. Clean peels were dried naturally by exposing them to sunlight, then they were dried by electrical oven at 50 °C until their weight was stable. After that, the dried peels were crushed using a domestic grinder until homogeneous dimensions were obtained. Sieve analysis was carried out for a sample of 20 g of crushed peels as shown in Table 1. The powdered lemon peels were stored in amber glass jars, protected from sunlight, and kept in a dry environment. For subsequent remediation experiments, peels that passed through a 45-mesh sieve were utilized.

2.2. Preparation of the selenium stock solution

To prevent interference from other substances and compounds commonly found in actual wastewater, the experiments for selenium removal were carried out using prepared aqueous solutions with known concentrations. Firstly, a stock solution was prepared by dissolving 2393 mg of sodium selenate (Na_2SeO_4) (99% purity, manufactured by SPECTRUM, USA) with a sufficient amount of distilled water in a 1 L graduated cylinder at laboratory temperature, with continuous stirring until all salt particles dissolved, and then the volume was completed to 1 l. Thus, the concentration of the resulting solution was 1000 ppm selenium.

2.3. Calibration curve

The selenium concentration was measured using a SHIMADZU AA-7000 Atomic Absorption Spectroscopy (AAS) device. Accurate concentration detection required the creation of a calibration curve, which was established at a wavelength of

Table 1. Lemon peels powder used in the study performed with a sieve analysis.

#	Sieve Size, (μm)	Mesh	Weight (g)	% wt
1	500	35	1.906	9.53
2	400	40	2.890	14.45
3	354	45	6.524	32.62
4	297	50	3.070	15.35
5	250	60	2.242	11.21
6	210	70	1.148	5.74
7	177	80	1.458	7.29
8	Pan	–	0.762	3.81
Σ	–	–	20 g	100%

196 nm. The slit width remained constant at 1 nm, and the working range varied from 0 to 200 ppm. The preparation of the calibration curve followed the guidelines in Ref. [55] and is illustrated in Fig. 1.

2.4. Adsorption unit

The selenium adsorption experiments using lemon peels were performed in a batch setup under various operating conditions. An adsorption unit, the Thermo Scientific MaxQ SHKE7000 Benchtop water bath shaker (Model 4303), equipped with 9 sample holders, was employed. Each 0.15 L borosilicate glass conical flask (IndiaMART, India) was filled with 100 cm^3 of selenium solution and a specific quantity of lemon peels, which was then placed in the water bath shaker. The pH of the Se^{+6} solution was adjusted using 0.1 N HCl or NaOH solutions. After setting the temperature, and agitation speed, the experiment was started and continued for the required time. The operating parameters were varied between 1 and 11, 100–500 rpm, 1–90 ppm, 5–180 min, 0.4–5.5 g, and 20–55 °C for the pH, agitation speed, initial concentration of selenium, time, dose of adsorbent, and temperature, respectively. The samples were then extracted carefully, and filtrated using a filtering unit (Filtering Kit 250 ml, Vacuum Pump with Gauge, KT3003-3 Science Lab Supplies/UK). The filtrate was analyzed using Atomic Absorption Spectroscopy (AAS) to determine the selenium concentration, which was quantified based on the calibration curve. The adsorption efficiency and capacity were calculated using Equations 1 and 2, respectively [27].

$$\%R = \frac{C_i - C_f}{C_i} \tag{1}$$

$$q = \frac{V(C_i - C_f)}{m} \tag{2}$$

2.5. Point of zero charge (pH_{PZC})

2.5.1. Preparation of the potassium nitrate solution

A 0.01 N potassium nitrate stock solution was meticulously prepared following stringent laboratory safety procedures. The preparation began with the precise measurement of 1.013 g of high-purity reagent-grade KNO_3, with a purity of 99.8%, obtained from MERCK-Germany. This measured quantity of potassium nitrate was then gradually dissolved in 1 L of double-distilled water, with a conductivity of 1.0 μS/cm, at room temperature. The solution was manually stirred until the entirety of the KNO_3 was completely dissolved.

2.5.2. Determination of the point of zero charge (pH_{PZC})

A series of 100 ml Pyrex™ Borosilicate Glass Erlenmeyer flasks, equipped with screw caps, were employed to prepare the suspension solutions. In each flask, 100 ml of 0.01 N KNO_3 solution –*prepared previously*-was introduced, and the pH of each solution was measured using (HI-83141-1 pH Meter,

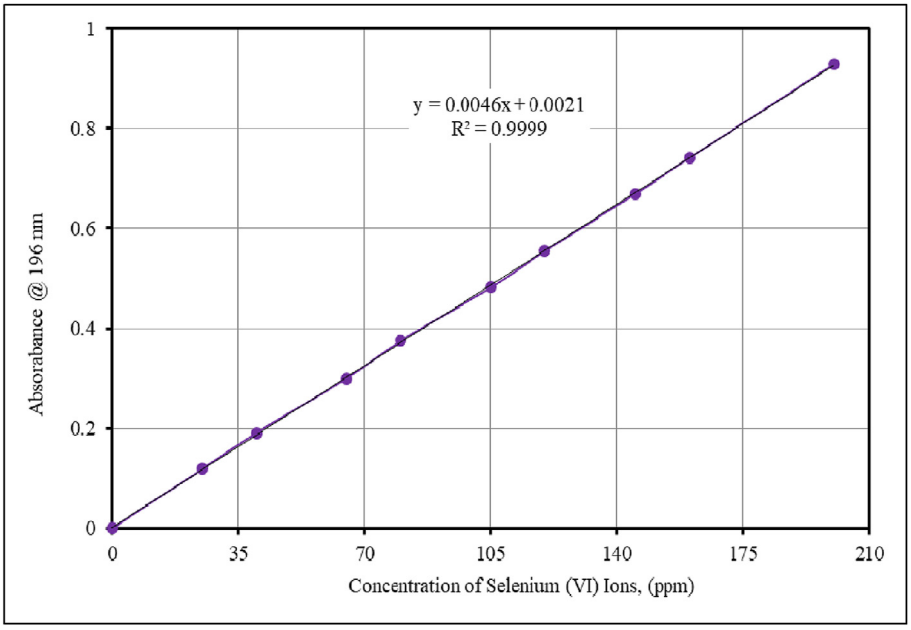

Fig. 1. Calibration curve of the selenium concentration using the Atomic Absorption Spectroscopy (AAS) device used in this study.

Hanna-USA) and accurately adjusted to span a range from pH 1 to 14. This adjustment was achieved by judiciously employing either 0.1 N HCl or NaOH solutions, establishing these pH values as the initial pH conditions. Subsequently, 1 g of finely ground lemon peel samples (45 mesh), which had been pre-dried, was added to each flask. This addition was conducted under controlled conditions, employing a hotplate magnetic stirrer (C-MAG MS 7, IKA™) operating at 200 rpm and ambient temperature. The stirring process was continued for a quarter of an hour to guarantee a uniform suspension. After the mixing process was completed, the flasks were immediately sealed with aluminum foil and secured with rubber bands to maintain consistent pH levels. To ensure uniform conditions throughout the experiment, the flasks containing the suspension were placed in an orbital water bath shaker and agitated overnight.

(Marshall Scientific Barnstead MaxQ 7000). This agitation was maintained at a constant temperature of 25 °C and an agitation speed of 100 rpm. Following 24 h equilibration period, the average pH values were determined based on five separate measurements of the liquid supernatant. These measurements were conducted to ensure the accuracy and reliability of the obtained pH_{PZC} value. The pH_{PZC} values were for determining the position where the resulting curves cut through the pH_o axis. For lemon peels, pH_{PZC} was recorded as 8. This value can be useful for predicting the surface charge of the adsorbents; when adsorption occurred at a particular pH below the point of zero charge of the adsorbent, the surface of the adsorbent will be positive, and will be negative when vice versa. The pH versus pH_{PZC} of the lemon peel is depicted in Fig. 2.

3. Results and discussion

3.1. Characterization of the adsorbent medium

3.1.1. FESEM test

The surface morphology of the adsorbent can be demonstrated using the field emission scanning electron microscopy (FESEM) image by FEI Inspected F-50, USA model. In the present study, the FESEM of lemon peel before selenium adsorption showed heterogeneous, rough and porous nature. However, after the adsorption of selenium, the surface is almost smooth and homogeneous in nature (Fig. 3a and b). The transformation of the surface of the lemon peels, transitioning from their initial heterogeneous, rough, and porous characteristics to a smooth and symmetric nature can be attributed to the process of adsorbing selenium. As the metal ions interact with the lemon peels' surface, they adhere to its irregularities and porous structures. This interaction leads to accumulating

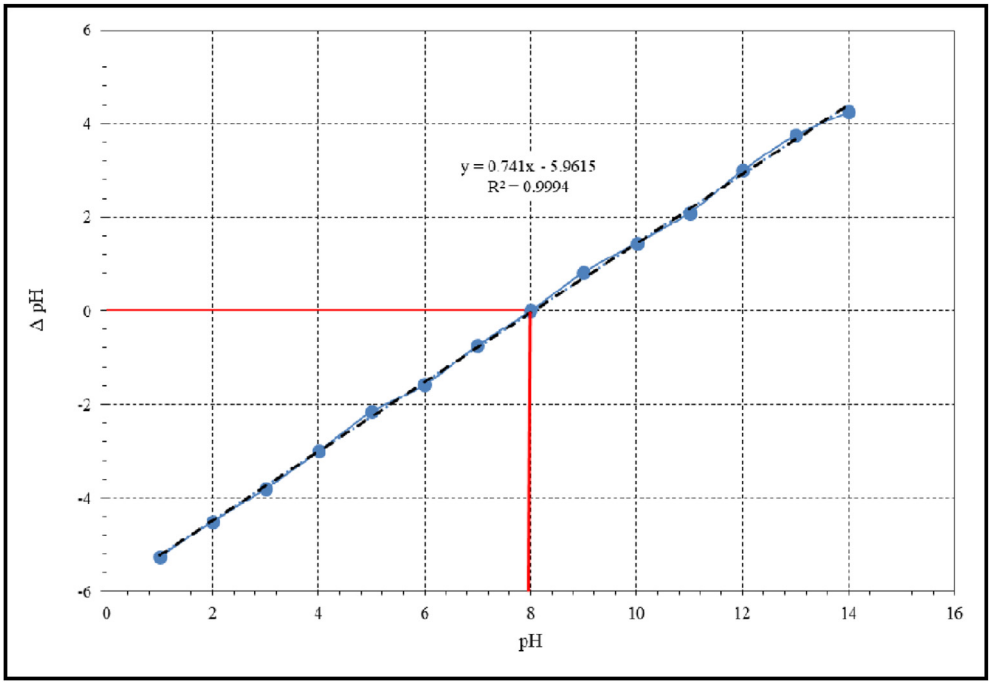

Fig. 2. pH_{ZPC} analysis of the lemon peels adsorbent.

a

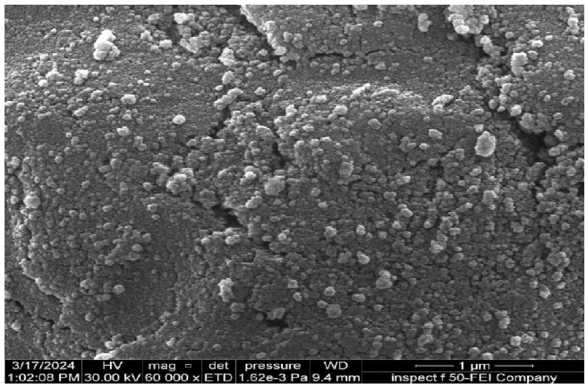

b

Fig. 3. a. FESEM test for lemon peels before adsorption. b. FESEM test for lemon peels after adsorption.

selenium ions in the pores and unevenness present on the surface of the adsorbent [21].

3.1.2. Specific surface area (S_{BET})

The surface area of the lemon peels was measured using N_2 physical adsorption-desorption at −77 K. Initially, the adsorption process filled the micro-pores at $P/P^{\circ} = 0.34513$, followed by the meso-pores with multiple layers of N2 gas. The surface area of the lemon peels was evaluated before and after selenium adsorption, yielding values of 27.86 m^2/g and 2.18 m^2/g, respectively, as shown in Fig. 4. The initial moderate surface area suggests a porous and rough structure, corroborated by FESEM analysis, that identified distinct pores on the lemon peel surface. After selenium adsorption, the surface area dropped to approximately 13.6% of the initial value. This substantial decrease indicates that a significant portion of the lemon peel's surface area was occupied by Se^{+6} ions [21].

3.1.3. FTIR test

Fig. 5 presents the FTIR spectra of the lemon peels both before and after the adsorption of selenium metal. The analysis was conducted using the FTIR device of IRPrestige-2, Shimadzu, specifically the Japan model and indicates that several peaks either disappeared or shifted due to the interaction with selenium, suggesting that lemon peels are effective adsorbents for heavy metals in general and

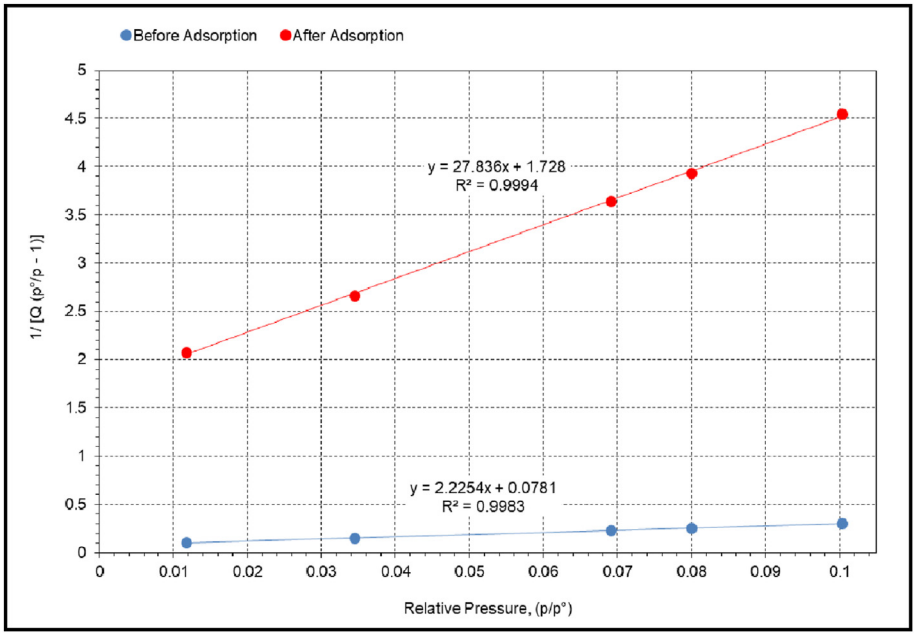

Fig. 4. BET surface area plot of the lemon peels.

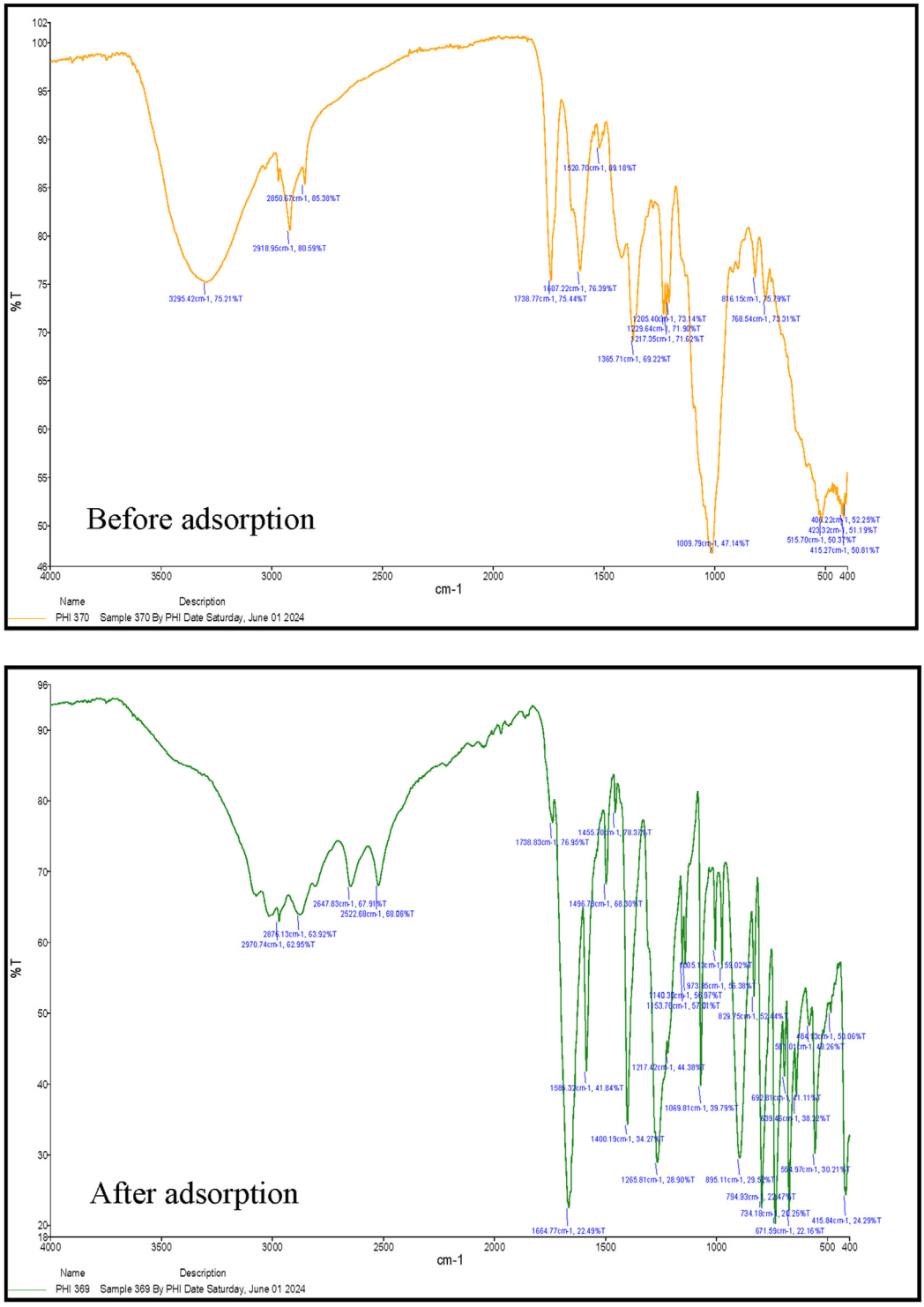

Fig. 5. FTIR spectrum of the lemon peels before and after adsorption of selenium ions.

selenium in particular. Before adsorption, the FTIR test recognized various peaks. The peak of 3295.42 cm^{-1} represents the O–H stretching vibrations, indicative of the hydroxyl groups in alcohols and phenols. The peaks of 2918.95 and 2850.67 cm^{-1} correspond to the C–H stretching vibrations in alkanes. The peak 1738.77 cm^{-1} is assigned to the C=O stretching vibrations in esters or carboxylic acids. The peak 1607.22 cm^{-1} is associated with the C=C stretching vibrations in aromatic rings. Peak

1520.7 cm^{-1} indicates the N–H bending vibrations in amines. Peak 1365.71 cm^{-1} represents the C–H bending vibrations. Peaks 1229.64, 1217.35, and 1205.4 cm^{-1} correspond to the C–O stretching vibrations in the alcohols, esters, or ethers. Peak 1009.79 cm^{-1} indicates the C–N stretching vibrations in the amines. Peaks 816.15, 768.54, 515.7, 423.32, 415.27, and 406.22 cm^{-1} represent the various bending and stretching vibrations typical for the structural components of lemon peels. After adsorption of the selenium, the lemon peels suffered from different changes and shifting in the original peaks. Peaks 2970.74, 2876.13, 2647.83, and 2522.68 cm^{-1} shift and new peaks in the C–H stretching region indicate changes in the hydrocarbon environment. Peak 1738.83 cm^{-1} underwent a slight shift in the C=O stretching vibrations, suggesting an interaction with selenium ions. Peaks 1664.77 and 1585.32 cm^{-1} represent shifts in the C=C and C=N stretching vibrations, implying a complex formation with selenium. Peaks 1469.78 and 1455.7 cm^{-1} change with the C–H bending vibrations. The 1400.19 cm^{-1} new peak indicates possible interactions with selenium. Peaks 1265.81, 1217.42, and 1153.76 cm^{-1} shift in the C–O stretching vibrations, showing alterations in the ester and ether groups. Peaks 1069.81, 1005.13, 973.85, and 895.11 cm^{-1} are both new and shifted peaks in the fingerprint region, indicating structural changes due to adsorption. The peaks 829.75, 794.93, 734.18, 692.81, 671.59, 639.46, 581.01, 554.97, 484.13, and 415.84 cm^{-1} represent various shifts in the bending and stretching vibrations, showing a significant interaction between the selenium ions and the functional groups of the lemon peels. The observed changes in positions of peaks and the appearance of new peaks after adsorption provide evidence of chemical interactions between selenium ions and the functional groups present in lemon peels. The shift and changes in the intensity of specific bands, such as the O–H, C=O, C=C, and C–O stretching vibrations, suggest the formation of new bonds and the complexation of selenium with the active sites on the lemon peels. The FTIR results further corroborate the findings from the FESEM analysis, demonstrating the chemical interactions between selenium and the functional groups located on the active sites across the surface of the peels.

These interactions played a pivotal role in the binding of selenium ions to the peels, which leads to the merging of the pores together and reduction in surface area. This result agrees with that of [56].

3.2. Effect of different operating parameters

3.2.1. Effect of acidity

To obtain the effect of pH on the adsorption efficiency of selenium ions using lemon peels as an adsorbent, a series of experiments were performed by changing the pH of the solution in the range 1–11, while keeping all other operating parameters constant at lab temperature alongside 10 g/L lemon peels, 1 ppm concentration, 300 rpm agitation speed and 180 min contact time. Fig. 6 shows that by increasing the pH from 1 to 8, the removal efficiency of selenium increased too from 7 to 72%

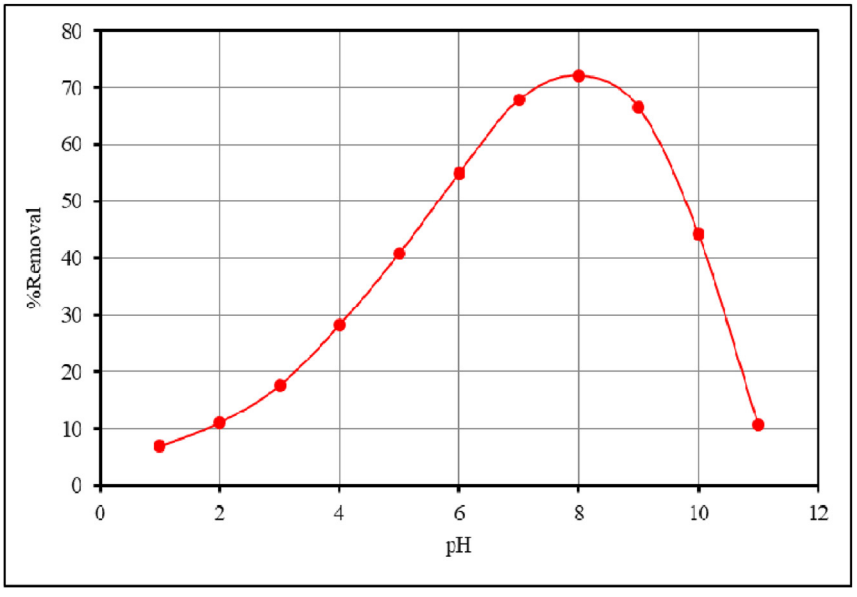

Fig. 6. Effect of acidity on selenium removal using lemon peels.

respectively, while dropping after that sharply to 10.6% at a pH of 12. Within the acidic range, the concentration of H^+ was high, as these ions cause repulsion and competition between them and the positive selenium ions regarding the active sites on the surface of the adsorbent material, so the adsorption efficiency was at its lowest value at pH = 1 where the concentration of hydrogen ions reached maximum value. As the pH value increases, the concentration of hydrogen ions begins to decrease, which allows the selenium ions to reach the active sites with less competition, thus the adsorption efficiency increases as the pH value increases. In the neutral range, the competition will be minimal, as a large number of selenium ions can bind with the functional groups in the adsorbent material, and therefore the concentration of ions in the solution will decrease, which increases the adsorption efficiency according to Equation 1. The decline in efficiency observed beyond the neutral zone can be attributed to the adsorbent material reaching a state of saturation, rendering it incapable of absorbing any additional selenium ions [33].

3.2.2. *Effect of agitation speed*

The influence of agitation speed on selenium-polluted aqueous solutions was investigated within a range of 100–400 rpm, while maintaining all other experimental conditions as constant: 10 g/L of lemon peels, 1 ppm selenium concentration, a pH of 8, and a contact time of 180 min at laboratory temperature. The results indicate a direct correlation between agitation speed and adsorption efficiency. This outcome can be attributed to the increased likelihood of lemon peels encountering selenium ions due to the enhanced diffusion within the solution. Higher agitation speeds facilitate the movement of ions to the active adsorption sites, resulting in a decreased concentration of selenium in the solution. Additionally, the increased agitation speed boosts the mass transfer rate, allowing selenium ions to reach the adsorbent surface more rapidly due to heightened kinetic energy. Notably, the adsorption efficiency improved fourfold when agitation speed was increased by a factor of 4.5. It is also clear that the obtained results represented in Fig. 7 indicate that the maximum value of adsorption occurs at an agitation speed of 450 rpm and then remains constant.

This result can be explained by the fact that the adsorption capacity of lemon peels has reached its maximum, as it is saturated and there is no ability to adsorb an additional amount of selenium ions. Therefore, it has become certain that 450 rpm is the optimal value for the adsorption of selenium ions by lemon peels [40].

3.2.3. *Effect of initial concentration of selenium*

The effect of the initial Se^{+6} concentration on adsorption efficiency was studied within the range of 1–90 ppm. All other parameters were maintained as constant: 20 °C, 10 g/L of adsorbent, 450 rpm, pH 8, and contact time of 3 h. The findings, illustrated in Fig. 8, revealed that the highest adsorption capacity

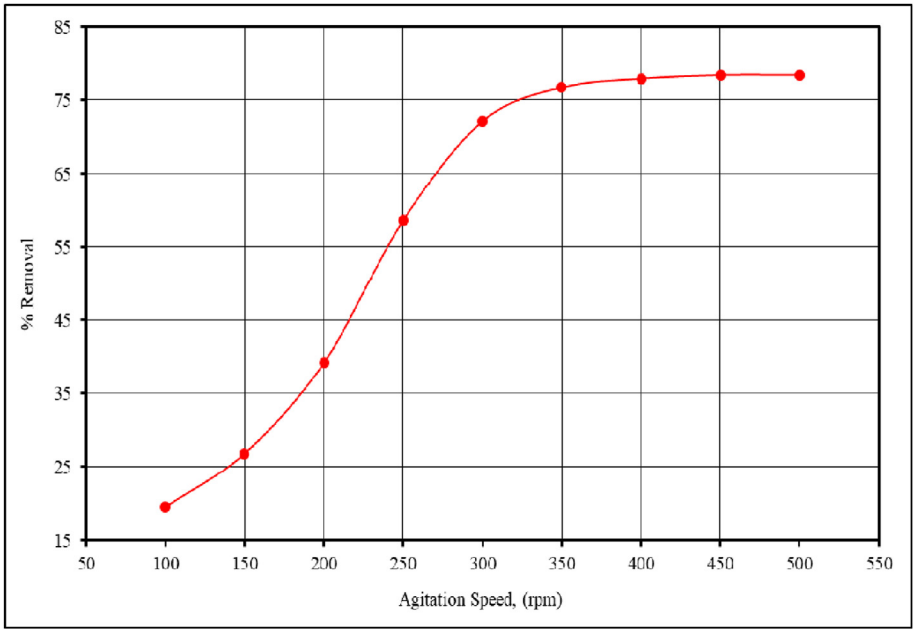

Fig. 7. Effect of agitation speed on selenium removal by lemon peels.

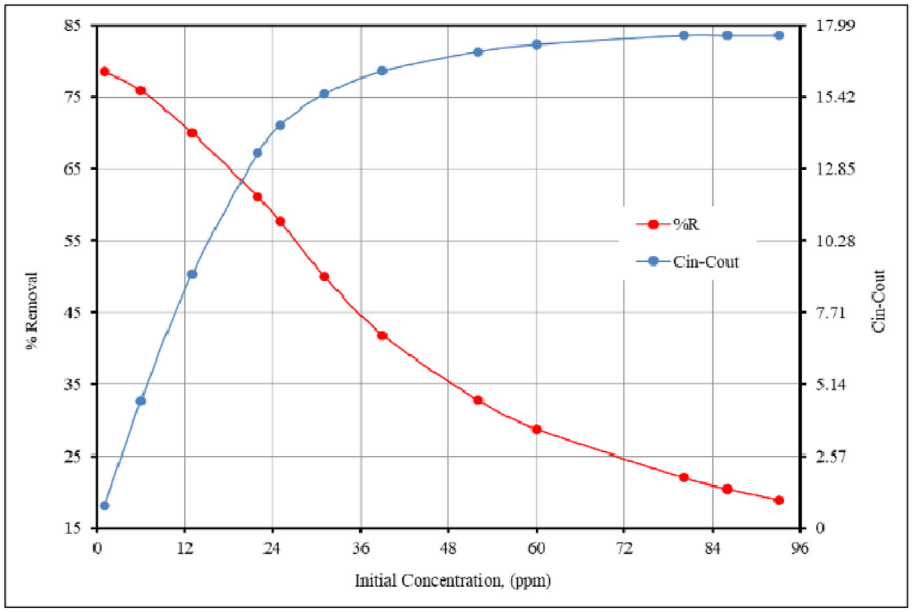

Fig. 8. Effect of initial concentration on removal efficiency.

of selenium was 17.6093 mg/g, achieved at an initial concentration of 86 ppm. This concentration was identified as the optimal initial concentration for the subsequent adsorption experiments. At lower concentrations, the selenium mass is minimal, allowing the adsorption medium to effectively absorb the heavy metal ions, enhancing the efficiency.

At high concentrations, the mass of Se^{+6} will be greater than it is in low concentrations, and the lemon peels will be able to adsorb a specific quantity of selenium ions, leaving the remaining ions free in the solution, meaning that the adsorption efficiency decreases. Additionally, Fig. 8 demonstrates a rise in the adsorbed concentration relative to the initial concentration. As the initial concentration increases, the adsorbed concentration will also increase until it stabilizes at a constant value, which represents the maximum capacity of the adsorbent for selenium ions [20].

3.2.4. Effect of adsorbent dose

Fig. 9 illustrates the adsorption behavior of selenium ions at varying adsorbent doses while maintaining other constant conditions: room temperature, an initial concentration of 86 ppm, an agitation speed of 450 rpm, a pH of 8, and a contact time of 180 min. The figure demonstrates a direct relationship between adsorption efficiency and the adsorbent dose within the range of 0.4–5.0 g. However, beyond 50 g/L, the removal efficiency remains unchanged at the optimal value of 87.648%, even with an increased adsorbent dose up to 55 g/L. As the dose increases, the surface area expands, leading to a higher number of functional groups available for binding with the selenium ions. This is due to the increased number of active sites distributed across the adsorption surface, resulting in enhanced adsorption efficiency. Concurrently, the adsorption capacity (q) diminishes, as illustrated in Fig. 9. This inverse relationship indicates that smaller amounts of adsorbent correlate with a higher adsorption capacity, as per the aforementioned Equation 2. It is noticed from Fig. 9 that the adsorption efficiency reached its maximum value at 50 g/L and remained constant without change because the peels cannot adsorb a further amount of Se^{+6} due to saturation [24].

3.2.5. Effect of contact time

The effect of contact time on the removal of selenium from an aqueous solution was examined within a range of 5–180 min. During this investigation, other parameters were maintained as constant: laboratory temperature, an initial concentration of 86 ppm, an agitation speed of 450 rpm, a pH of 8, and 50 g/L of lemon peels. The outcomes of these conditions are illustrated in Fig. 10, showing the relationship between varying contact times and the corresponding adsorption efficiency. It is evident that there is a direct relationship between these variables, with adsorption efficiency increasing from 6.25% at 5 min to 87.648% at 150 min, after which it remained constant. Increasing the time of the

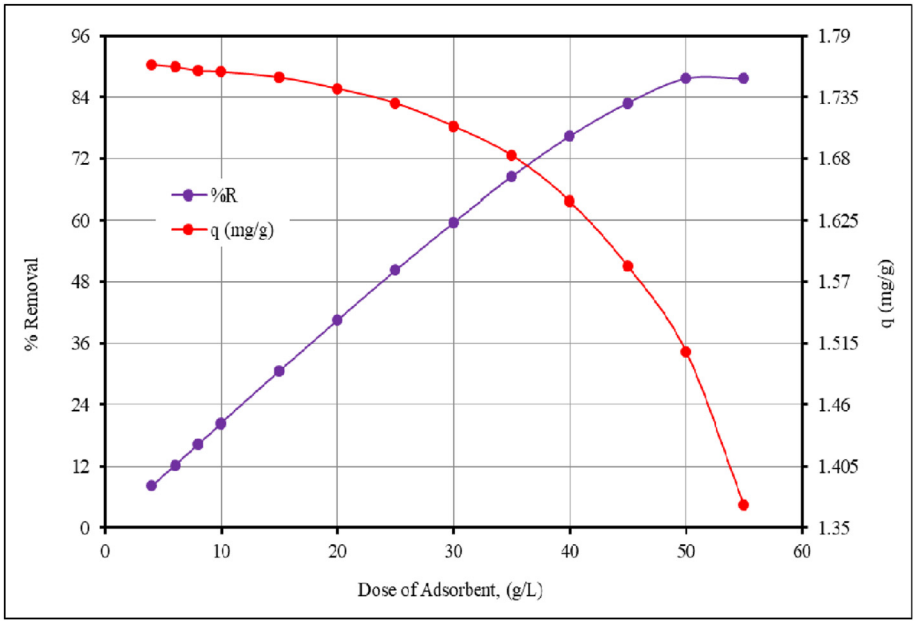

Fig. 9. Effect lemon peels on selenium removal.

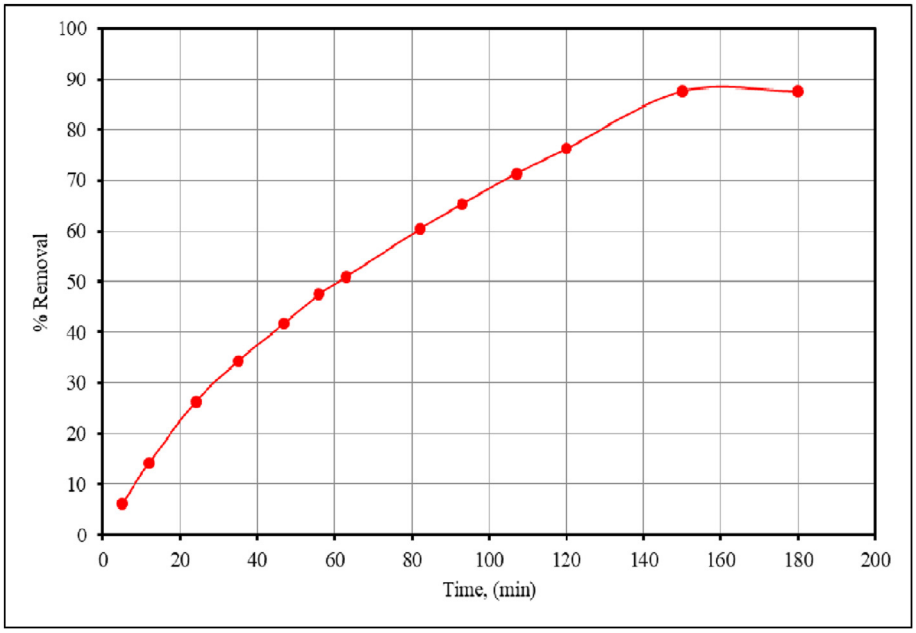

Fig. 10. Effect of contact time on selenium removal using lemon peels.

adsorption process provided additional time to adsorb a great number of Se^{+6} on the surface of the lemon peels. There will be a greater opportunity for more ions to reach the active sites on the adsorption surface, which in turn leads to an increase in the efficiency of the adsorption process. It is also noted that the efficiency and capacity of adsorption remained constant after 150 min without change, and the reason for this is that the material at this time has reached the level of saturation at the current operating conditions [29].

3.2.6. *Effect of temperature*

The effect of the adsorption unit temperature was explored in the range between 20 and 50 °C, while the other operating variables were kept constant at their optimum values, i.e. 50 g/L, 8, 450 rpm, 86 ppm, and 150 min for the dose of lemon peels,

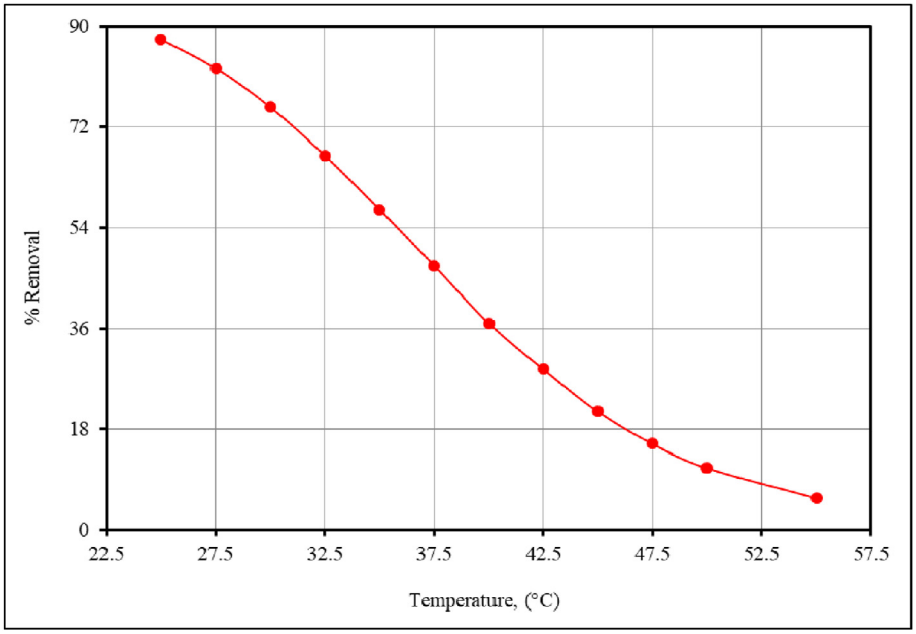

Fig. 11. Effect of temperature on selenium removal using lemon peels.

pH, agitation speed, the initial concentration of selenium ions and contact time, respectively. It's clear from Fig. 11, which explains the experimental results of changing the temperature, that there was an inverse relation between the temperature values and selenium removal, and that the maximum efficiency of adsorption performed at 20 °C. The rise in temperature resulted in a higher kinetic energy for the selenium ions, causing them to move away from the adsorption surface and remain free in the solution. It may have supplied the necessary energy for the ions to break free from the binding forces of the functional groups at the active sites. This finding indicates that the selenium adsorption process is more efficient at lower temperatures. Specifically, an adsorption efficiency of 87.648% was recorded at 20 °C, whereas the efficiency significantly dropped to 5.756% at 50 °C. The behavior of temperature in the study of [30] is consistent with the results of the current study.

4. Adsorption behavior

In the adsorption processes the adsorption isotherm calculation is essential, as it detects the relationship at a constant temperature between the amount of adsorbent (q_e) and the surface equilibrium concentration of the adsorbent (C_e). This calculation helps in understanding and evaluating the efficiency of the adsorbents, as well as determining adsorption mechanism, and proposing industrial adsorption systems. However, the adsorption performance can be predicted through the adsorption isotherm analysis under different conditions, which can improve the use of adsorbents and reduce the cost. There are several models used to illustrate the adsorption isotherm of adsorption. The isotherm models used in the present study are the Langmuir, Temkin, Freundlich, and renowned models [21].

4.1. The Langmuir isotherm model

This model assumes that the energy of all adsorbed cites on the surface is constant, and that adsorption occurs in a monolayer, completely occupying all available surface positions. Moreover, it is assumed that there are no intermolecular interactions among the molecules that are adsorbed onto the surface.

This assumption is presented by combining the presence of a dynamic equilibrium between the adsorbed molecules and the molecules appearing in the gaseous or liquid phase. Equations 3–5 describe the mathematical relations of this model [56].

$$q_e = \frac{q_{max}.K_L C_e}{1 + K_L C_e} \tag{3}$$

$$\frac{1}{q_e} = \frac{1}{q_{max} K_L}\frac{1}{C_e} + \frac{1}{q_{max}} \tag{4}$$

$$R_L = \frac{1}{1 + K_L C_e} \tag{5}$$

4.2. The Freundlich isotherm model

This model depends on the assumption that the surface of the adsorbent is heterogeneous, with the implication that there are different types of adsorbent position with different level of adsorption energies, and also that adsorption can occur in multiple layers, and the energy level of adsorption is varies. This means that molecules can adsorb not only on the surface of the adsorbent but also on previous molecules that were adsorbed. Eventually, this model implies the presence of a dynamic state of balance between the molecules that are present in the solution and the molecules that are attached to the surface at a stable temperature [27]. Equations 6 and 7 describe the mathematical relations of this model.

$$q_e = K_F C_e^{\frac{1}{n}} \tag{6}$$

$$\ln q_e = \ln K_F + \frac{1}{n} \ln C_e \tag{7}$$

4.3. Temkin isotherm model

This model proposes that due to the interactions between the adsorbent, the latent heat of adsorption decreases linearly with the increase the coverage of the surface. This model focuses on certain fundamental assumptions that make it ideal for understanding adsorption in specific systems. Firstly, it requires the existence of interactions between the adsorbed molecules, which consequently results in the modification of the adsorption energy as the quantity of adsorbed molecules grows [56]. Equations 8 and 9 describe the mathematical relations of this model.

$$q_e = \frac{RT}{b} \ln K_T C_e \tag{8}$$

$$q_e = \frac{RT}{b} \ln K_T + \frac{RT}{b} \ln C_e \tag{9}$$

Figs. 12–14 show the isotherm models of Langmuir, Freundlich and Temkin for the lemon peels used for the adsorption of selenium ions constants, while Table 2 shows the values of the isotherm models used in the current study. The data show that the degree of agreement of the experimental results with these models takes the form of Langmuir > Timkin > Freundlich models for selenium ions according to the value of the correlation coefficient, which was 0.9996, 0.941 and 0.9312 respectively. It is clear that the adsorption process of selenium ions using lemon peels as an adsorbent is subject to Langmuir's isotherm better than other models due to the high correlation coefficient value. This means that the adsorption occurs on a

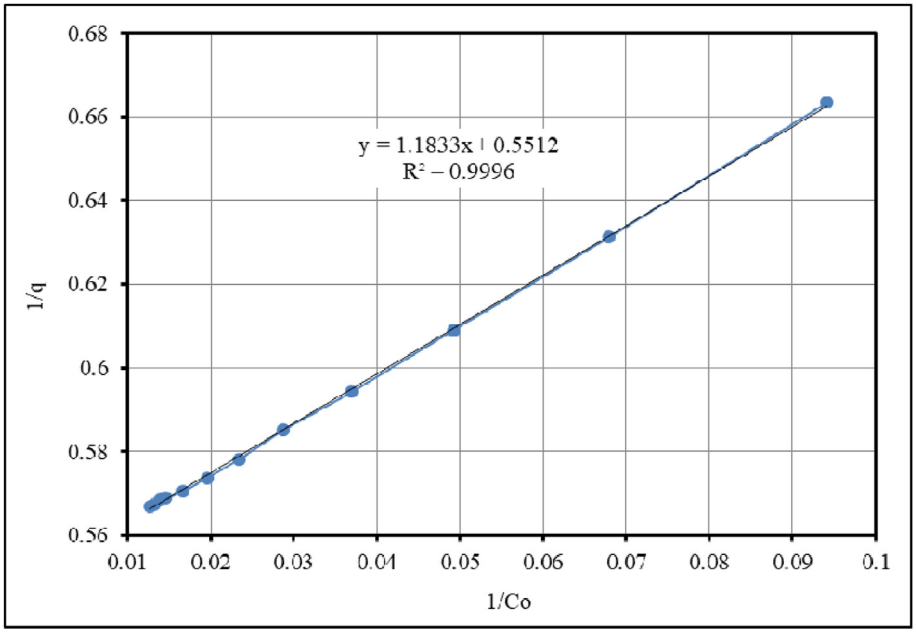

Fig. 12. Langmuir model.

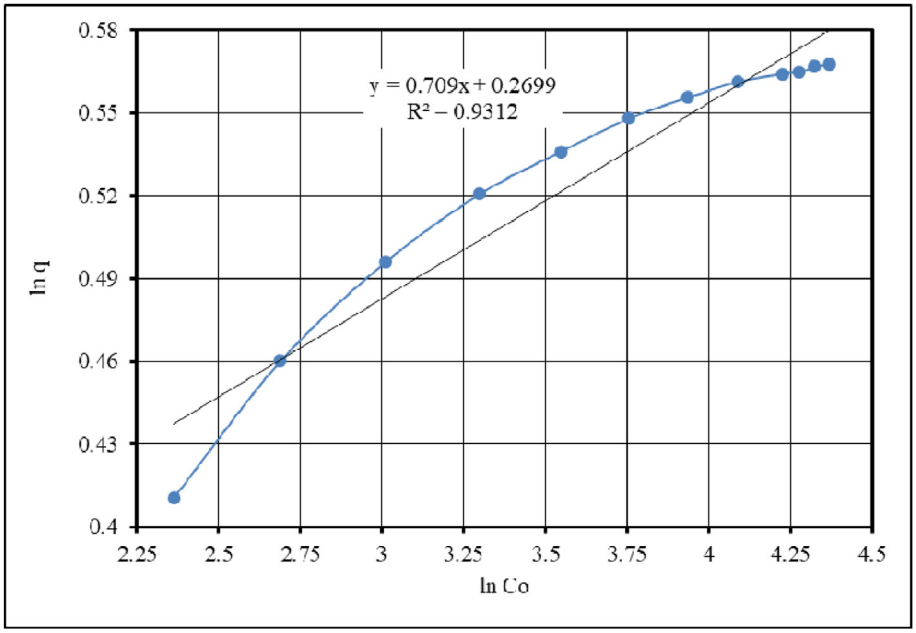

Fig. 13. Freundlich model.

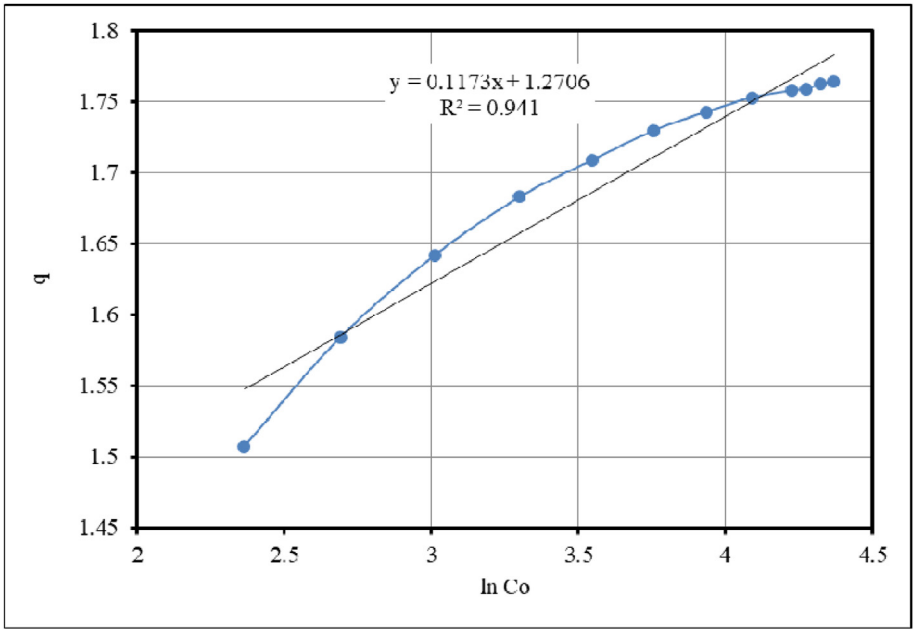

Fig. 14. Temkin model.

monolayer surface with a finite number of identical sites, and that the adsorption process is preferred according to the value of the separation factor, which was 0.0075.

5. Adsorption kinetics

To estimate adsorption kinetics several mathematical models have been employed, including the pseudo-first-order model, the pseudo-second-order model, Elovich model, and the intra-particle diffusion model. By employing these models, it is possible to further improve the efficacy of adsorption and it is associated with a lower operational cost. This in turn, contributes to the optimization of adsorption technologies to achieve optimal efficiency in removing the pollutants and significant improvement [25].

Table 2. The constants values of isotherm models used in the current study.

Model	Parameter	Value
Langmuir	q_{max}	1.8142
	k_L	1.5332
	R_L	0.0075
	R^2	0.9996
Temkin	b	20,768
	k_T	5.0617
	R^2	0.941
Freundlich	k_F	1.3098
	n	1.4067
	R^2	0.9312

5.1. Pseudo-first-order model

According to this model, adsorption occurs in a medium with constant temperature and pressure. The molecules that are adsorbed do not interact with each other on the surface, demonstrating that adsorption occurs regardless of other concentrations. Equations 10 and 11 describe the mathematical relations of this model [57].

$$\frac{q_t}{q_e} = 1 - e^{-k_1 t} \tag{10}$$

$$\ln(q_e - q_t) = \ln q_e - k_1 t \tag{11}$$

5.2. Pseudo-second-order model

This model proposes that the adsorption rate is directly proportional to the square of the difference between the equilibrium concentration and the concentration at any time given. This model indicates that all active sites on the adsorbent surface are both available and consistent, and that they sustain their efficiency throughout the whole adsorption process. A crucial hypothesis of this model argues that adsorption contains both a chemical reaction and electronic exchange between the adsorbed molecules and the active sites on the adsorbed surface. Chemical adsorption occurs when strong chemical bonds are formed between the adsorbent and the adsorbent surface. However, for adsorption caused by a chemical mechanism this type of adsorption is considered appropriate. Equations 12 and 13 describe the mathematical relations of this model [57].

$$\frac{q_t}{q_e} = (q_e - q_t) k_2 t \tag{12}$$

$$\frac{t}{q_t} = \frac{1}{k_2 q_e^2} + \frac{t}{q_e} \tag{13}$$

5.3. Elovich model

The assumptions of the Elovich model are based on the fact that the adsorption or reaction process occurs in a sequence of steps in which the state of the surface or its reaction is changed, and the rate of adsorption or reaction changes with time and is affected by factors such as changing the concentration of compounds adsorbed on the solid surface. The model also assumes that adsorbed or reacting molecules are continuously replaced on the solid surface, leading to continuous changes in the rate of reaction or adsorption. It is assumed that changes in the solid surface significantly affect the rate of reaction or adsorption [5]. The mathematical relations of this model is highlighted by equations 14 and 15.

$$q_t = \frac{1}{\beta} e^{\alpha\beta t} \tag{14}$$

$$q_t = \frac{1}{\beta} \ln \alpha\beta + \frac{1}{\beta} \ln t \tag{15}$$

5.4. Intra-particle diffusion model

The model assumes that the adsorption rate can be controlled by the primary factor of intra-molecular diffusion. This implies that the transportation of molecules inside the pores of the adsorbent material indicates the slowest stage in the adsorption process. Moreover, it is expected that the diffusion takes place uniformly throughout these pores whereas the adsorbent maintains uniform and consistent pores. Furthermore, the model expects that the motion of molecules occurs via the pores, influenced by a concentration gradient, where the molecules move from higher concentration to lower concentration regions [29]. Equation 16 represents the mathematical relation of this model.

$$q_t = k_d \sqrt{t} + C \tag{16}$$

The results of the kinetic study are represented by Figs. 15–18 and Table 3 indicating that the intra-particle diffusion model yielded the best fit to the experimental data having compared the other aforementioned models. The correlation coefficient (R^2) for this model was found to be 0.9993, which suggests a very strong agreement between the predicted values and the actual experimental observations. The higher significant correlation coefficient obtained for the intra-particle diffusion model

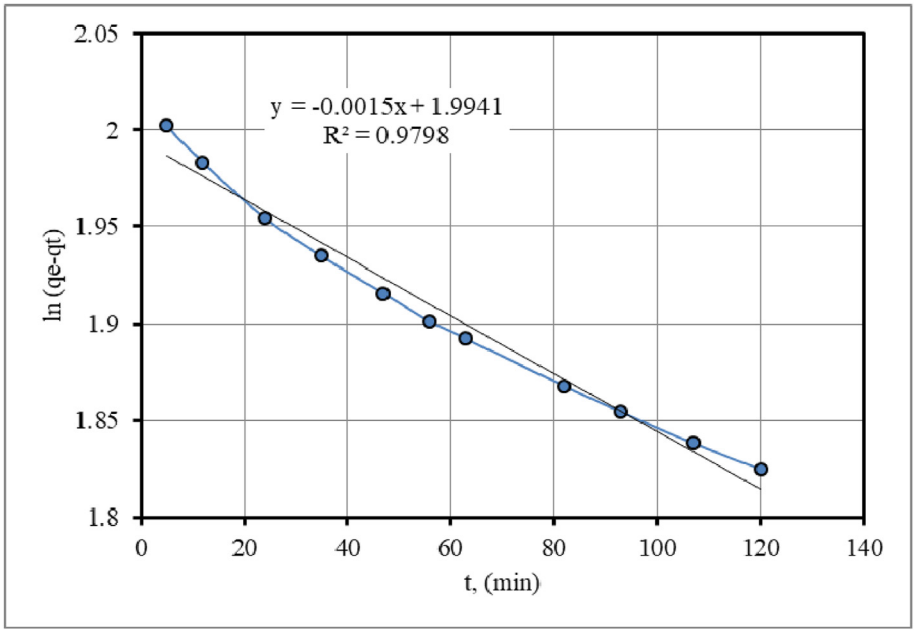

Fig. 15. Pseudo-first-order model.

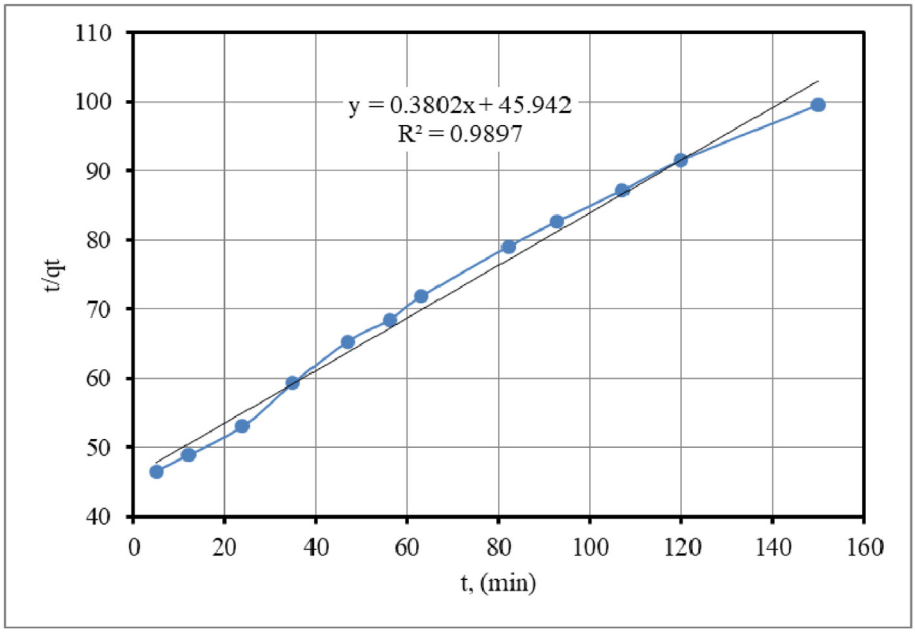

Fig. 16. Pseudo-second-order model.

indicates that this model accurately reflects the observed adsorption performance.

This suggests that the speed at which selenium ions spread across the porous structure of lemon peels has a significant impact on the whole adsorption process. However, the pseudo first order, pseudo second order, and Elovich models indicate the correlations with lower values of 0.9798, 0.9897, and 0.9308, respectively.

6. Adsorption thermodynamic

For determining the spontaneity, enthalpy, and randomness degree of the adsorption process, the thermodynamic functions must be calculated. A process is spontaneous if the value of ΔG is negative. When the enthalpy (ΔH) change is less than 40 kJ/mol, the adsorption is physical, whereas if the enthalpy changes over 80 kJ/mol, the adsorption is

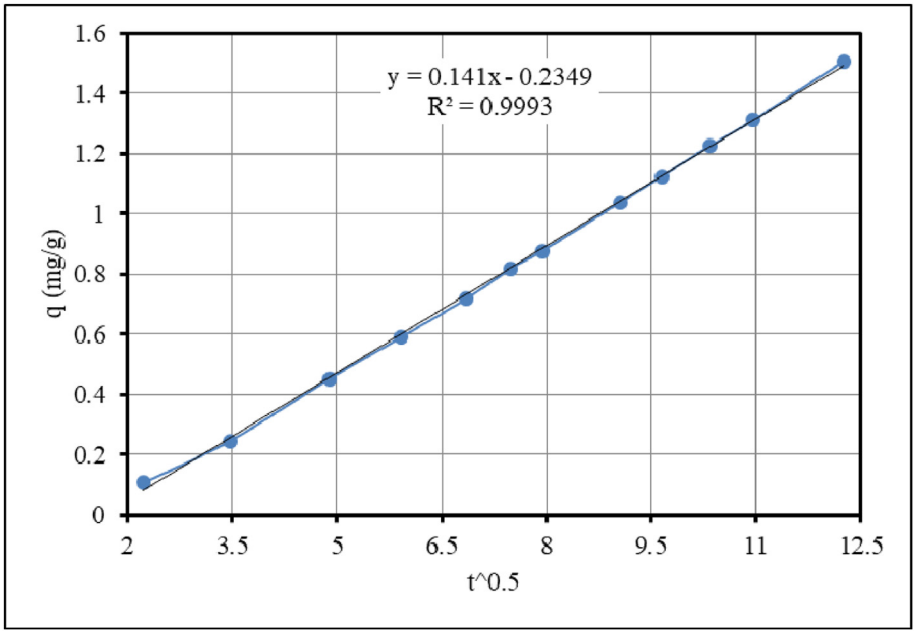

Fig. 17. Intra-particle diffusion model.

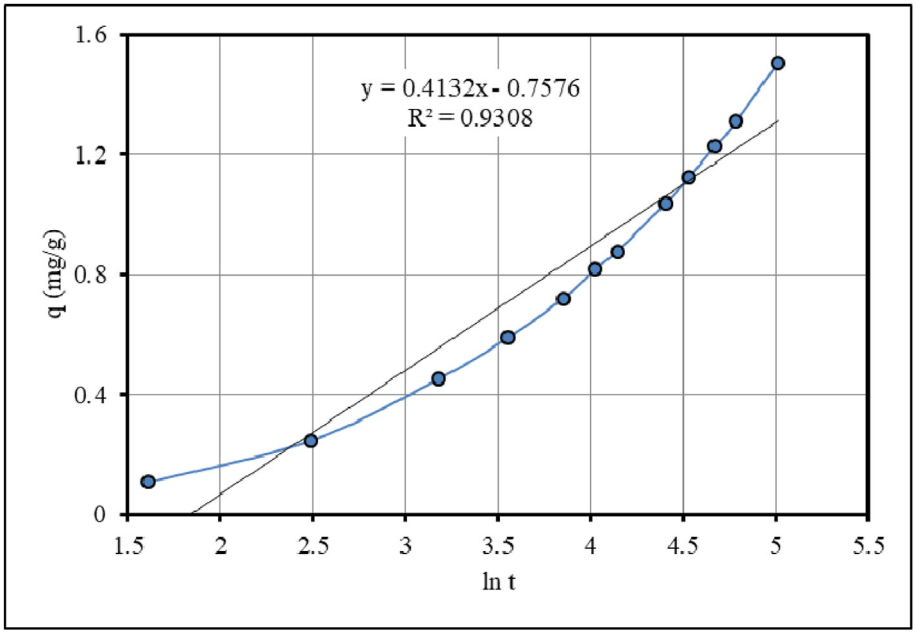

Fig. 18. Elovich model.

classified as chemical. The change in entropy (ΔS) can be analyzed to determine the degree of randomness resulting from adsorption. A positive ΔS value indicates an increase in randomness, while a negative value indicates a decrease in randomness. The calculation of the values of the thermodynamic functions is based on the Van-'t-Hoff equation, which is mathematically represented by Equation 18, where the adsorption equilibrium coefficient (k_{ad}) can be calculated from Equation 19 [56].

$$\ln k_{ad} = \frac{\Delta S}{\mathbb{R}} - \frac{\Delta H}{\mathbb{R}}\left(\frac{1}{T}\right) \tag{17}$$

$$k_{ad} = \frac{q_e}{C_e} \tag{18}$$

$$\ln k_{ad} = -\frac{\Delta G}{\mathbb{R}}\left(\frac{1}{T}\right) \tag{19}$$

Table 3. The constants values of the kinetics models used in the current study.

Model	Parameter	Value
Pseudo-first order	q_e	7.3456
	k_1	0.0015
	R^2	0.9798
Pseudo-second order	q_e	2.6302
	k_2	0.0031
	R^2	0.9897
Intra-particle diffusion	k_p	0.1410
	I	−0.2349
	R^2	0.9993
Elovich	α	0.0661
	β	2.4201
	R^2	0.9308

Table 4. Thermodynamic Behaviors of phenol adsorption using mandarin peels.

T (°C)	$\Delta H°$ (kJ/mol)	$\Delta S°$ (kJ/mol.K)	$\Delta G°$ (kJ/mol)
25	−129.7971	−381.6588	−16.0055
27.5			−15.0514
30			−14.0972
32.5			−13.1431
35			−12.1889
37.5			−11.2348
40			−10.2806
42.5			−9.3265
45			−8.3723
47.5			−7.4182
50			−6.4640
55			−4.5557

From Fig. 19 and Table 4, it can be seen that the adsorption is spontaneous, chemical type, exothermic and of decreased entropy, according to the value of enthalpy and the sign of ΔG, ΔH, and ΔS, respectively.

7. Comparison between this study and other studies

While the current manuscript is concerned with studying the ability of lemon peels to remove selenium from polluted aqueous solutions, various papers have delved into the possibility of removing selenium ions from contaminated water using different adsorbents, and also recovery following of different contaminants by lemon peels. Table 5 presents a comparative analysis of the findings

Table 5. Summary of different pollutants adsorbed by lemon peels and selenium adsorption using various adsorbents.

Adsorbent	Adsorbate	q, (mg/g)	Reference
Lemon peel	CN^-	1.472	[54]
Lemon peel	Zn^{+2}	3.048	[24]
Modified-lemon peel	Co^{+2}	3.57	[56]
Modified-lemon peel	Cr^{+3}	8.84	[56]
Modified-lemon peel	Cu^{+2}	2.22	[56]
Modified-lemon peel	Mn^{+2}	6.09	[56]
Modified-lemon peel	Pb^{+2}	3.16	[56]
Alkali-modified lemon peel	Ni^{+2}	0.626	[57]
Alkali-modified lemon peel	Cd^{+2}	0.726	[57]
Citrus peels	Se^{+4}	4.6	[7]
Wheat Bran	Se^{+6}	0.08065	[58]
Wheat Bran	Se^{+4}	0.08928	[58]
Egg shell membrane	Se^{+6}	37	[58]
Broiler chicken feathers	Se^{+6}	20.7	[59]
Lemon peel	Se^{+6}	1.8142	This study

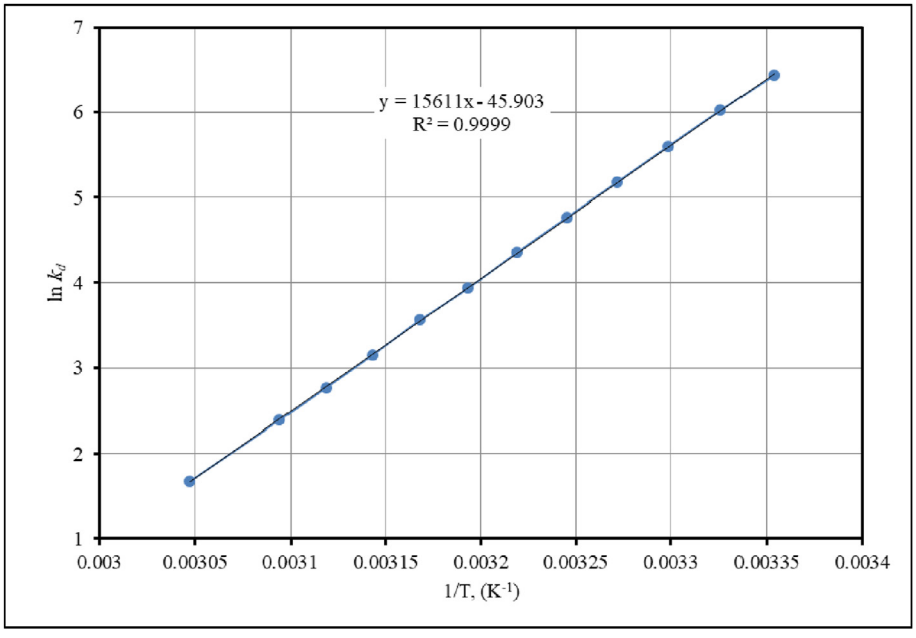

Fig. 19. Thermodynamic properties of selenium adsorption using lemon peels.

between this study and previous studies conducted by different researchers.

8. Conclusions

The most important finding of the current study is the ability of lemon peels to adsorb heavy metals in general and selenium in particular with high efficiency. The study showed that the highest removal efficiency of selenium ions was 87.648% and that it was achieved at a pH, agitation speed, initial concentration, adsorbent dose, contact time, and temperature of 8, 450 rpm, 86 ppm, 50 g/L, 150 min, and 20 °C, respectively, while the maximum capacity value of pomegranate peel to absorb selenium was 1.8142 mg/g. The results of the isotherm study confirmed that adsorption applied to the Langmuir model worked better than the other models, while the intra-particle diffusion model was the best for describing the adsorption kinetics. According to the thermodynamic study, it was found that the adsorption is spontaneous, exothermic, of a chemical type, and with decreasing entropy. Morphological investigations, including BET, FTIR, pH_{PZC} and FESEM analyses on both pristine and loaded lemon peels, illustrated the impact of selenium adsorption on pore closure. The BET analysis indicates that the adsorption process occupies more than 92% of the surface area post-treatment, and FTIR results highlight the disappearance and shift of numerous peaks, emphasizing the significant role of adsorption. The FESEM observations elucidate the closure of pores within the lemon peels due to selenium adsorption.

Acknowledgements

The authors would like to thank Mustansiriyah University (www.uomustansiriyah.edu.iq) Baghdad – Iraq; Kerbala University (www.uokerbala.edu.iq) Kerbala – Iraq; the University of Diyala (www.uodiyala.edu.iq) Diyala – Iraq; and Mutah University (https://mutah.edu.jo) Al Karak, Jordan.

References

[1] A.A. Zamani, M.R. Yaftian, A. Parizanganeh A, Multivariate statistical assessment of heavy metal pollution sources of groundwater around a lead and zinc plant, Iran J Environ Health Sci Eng 9 (2012) 1–10, https://doi.org/10.1186/1735-2746-9-29.

[2] M. Villen-Guzman, D. Gutierrez-Pinilla, C. Gomez-Lahoz, C. Vereda-Alonso, J.M. Rodriguez-Maroto, B. Arhoun, Optimization of Ni (II) biosorption from aqueous solution on modified lemon peel, Environ Res 179 (2019) 1–123, https://doi.org/10.1016/j.envres.2019.108849.

[3] M.N. Abbas, S.T. Ali, R.S. Abbas, Rice husks as a biosorbent agent for Pb^{+2} ions from contaminated aqueous solutions: a review, Biochem Cell Arch 20 (2020) 1813–1820, https://doi.org/10.35124/bca.2020.20.1.1813.

[4] D. Witkowska, J. Słowik, K. Chilicka, Heavy metals and human health: possible exposure pathways and the competition for protein binding sites, Molecules 26 (2021) 1–16, https://doi.org/10.3390/molecules26196060.

[5] M.S. Al Shammari, H.M. Ahmed, F.M. Abdel-Haleem, N.J. Almutlq, M.A. El-Khateeb, Adsorption of Chromium, Copper, Lead, Selenium, and Zinc ions into ecofriendly synthesized magnetic iron nanoparticles, PLoS One 18 (2023) 1–23, https://doi.org/10.1371/journal.pone.0289709.

[6] G.A.A. Ali, M.N. Abbas, Atomic spectroscopy technique employed to detect the heavy metals from Iraqi waterbodies using natural bio-filter (*Eichhornia crassipes*) thera dejla as a case study, sys, Rev Pharm 11 (2020) 264–271, https://doi.org/10.31838/srp.2020.9.43.

[7] S. Dev, A. Khamkhash, T. Ghosh, S. Aggarwal, Adsorptive removal of Se (IV) by citrus peels: effect of adsorbent entrapment in calcium alginate beads, ACS Omega 5 (2020) 17215–17222, https://doi.org/10.1021/acsomega.0c01347.

[8] M. Kieliszek, Selenium - fascinating microelement, properties and sources in food, Molecules 24 (2019) 1298, https://doi.org/10.3390/molecules24071298.

[9] H. Ullah, L. Lun, A. Rashid, N. Zada, B. Chen, A. Shahab, P. Li, M.U. Ali, S. Lin, M.H. Wong, A critical analysis of sources, pollution, and remediation of selenium, an emerging contaminant, Environ Geochem Health 45 (2023) 1359–1389, https://doi.org/10.1007/s10653-022-01354-1.

[10] World Health Organization (WHO), Selenium in drinking water, 2011. Retrieved from: http://www.who.int/water_sanitation_health/dwq/chemicals/selenium.pdf.

[11] Iraqi Quality Specification of Drinking Water-First Modernization (IQS-417), The Council of Ministers, Central Organization for Standardization and Quality Control (COSQC), 2001. IQS/417/2001[*in Arabic*].

[12] T. Zeng, Q. Hu, X. Zhang, H. Nong, A. Wang, Biological removal of Se and Cd from acidic selenite- and cadmium-containing wastewater with limited carbon availability, Bull Environ Contam Toxicol 107 (2021) 1208–1219, https://doi.org/10.1007/s00128-021-03302-8.

[13] R. Vidu, E. Matei, A.M. Predescu, B. Alhalaili, C. Pantilimon, C. Tarcea, C. Predescu, Removal of heavy metals from wastewaters: a challenge from current treatment methods to nanotechnology applications, Toxics 8 (2020) 1–37, https://doi.org/10.3390/toxics8040101.

[14] H. Elbasiouny, M. Darwesh, H. Elbeltagy, F.G. Abo-Alhamd, A.A. Amer, M.A. Elsegaiy, I.A. Khattab, E.A. Elsharawy, F. Ebehiry, H. El-Ramady, E.C. Brevik, Ecofriendly remediation technologies for wastewater contaminated with heavy metals with special focus on using water hyacinth and black tea wastes: a review, Environ Monit Assess 193 (2021) 1–19, https://doi.org/10.1007/s10661-021-09236-2.

[15] H.N. Hamad, S. Idrus, Recent developments in the application of bio-waste-derived adsorbents for the removal of methylene blue from wastewater: a review, Polymers 14 (2022) 1–39, https://doi.org/10.3390/polym14040783.

[16] B. Wang, J. Lan, C. Bo, B. Gong, J. Ou, Adsorption of heavy metal onto biomass-derived activated carbon: review, RSC Adv 13 (2023) 4275–4302, https://doi.org/10.1039/d2ra07911a.

[17] S.Y. Hwang, G.B. Lee, J.H. Kim, B.U. Hong, J.E. Park, Pretreatment methods for regeneration of spent activated carbon, Molecules 25 (2020) 1–10, https://doi.org/10.3390/molecules25194561.

[18] A.I. Osman, J.K. Abu-Dahrieh, M. McLaren, F. Laffir, P. Nockemann, D. Rooney, A facile green synthetic route for the preparation of highly active γ-Al2O3 from aluminum foil waste, Sci Rep 7 (2017) 1–11, https://doi.org/10.1038/s41598-017-03839-x.

[19] K. Li, P. Li, J. Cai, A. Li, Efficient adsorption of both methyl orange and chromium from their aqueous mixtures using a quaternary ammonium salt modified chitosan magnetic

composite adsorbent, Chemosphere 154 (2016) 310–318, https://doi.org/10.1016/j.chemosphere.2016.03.100.
[20] S. Giraldo, N.Y. Acelas, R. Ocampo-Pérez, E. Padilla-Ortega, E. Flórez, C.A. Franco, F.B. Cortés, A. Forgionny, Application of orange peel waste as adsorbent for methylene blue and Cd^{2+} simultaneous remediation, Molecules 27 (2022) 1–17, https://doi.org/10.3390/molecules27165105.
[21] S.J. Alhamd, M.N. Abbas, H.J.J. Al-Fatlawy, T.A. Ibrahim, Z.N. Abbas, Removal of phenol from oilfield produced water using non-conventional adsorbent medium by an eco-friendly approach, KIJOMS 10 (2024) 191–210, https://doi.org/10.33640/2405-609X.3350.
[22] N. Priyantha, H.K.W. Sandamali, T.P.K. Kulasooriya, Sodium hydroxide modified rice husk for enhanced removal of copper ions, Water Sci Technol 78 (2018) 1615–1623, https://doi.org/10.2166/wst.2018.395.
[23] W.A.H. Altowayti, N. Othman, A. Al-Gheethi, N.H.B.M. Dzahir, S.M. Asharuddin, A.F. Alshalif, I.M. Nasser, H.A. Tajarudin, F.A.H. Al-Towayti, Adsorption of Zn^{2+} from synthetic wastewater using dried watermelon rind (D-WMR): an overview of nonlinear and linear regression and error analysis, Molecules 26 (2021) 1–23, https://doi.org/10.3390/molecules26206176.
[24] A. Bondarev, D.R. Popovici, C. Călin, S. Mihai, E.E. Sîrbu, R. Doukeh, Black tea waste as green adsorbent for nitrate removal from aqueous solutions, Materials 16 (2023) 1–25, https://doi.org/10.3390/ma16124285.
[25] Q. Zaib, D. Kyung, Optimized removal of hexavalent chromium from water using spent tea leaves treated with ascorbic acid, Sci Rep 12 (2022) 1–14, https://doi.org/10.1038/s41598-022-12787-0.
[26] M. Khanna, A. Mathur, A.K. Dubey, J. McLaughlin, I. Moirangthem, S. Wadhwa, D. Singh, R. Kumar, Rapid removal of lead(II) ions from water using iron oxide-tea waste nanocomposite - a kinetic study, IET Nanobiotechnol 14 (2020) 275–280, https://doi.org/10.1049/iet-nbt.2019.0312.
[27] A. El-Sikaily, A. El Nemr, A. Khaled, O. Abdelwehab, Removal of toxic chromium from wastewater using green alga *Ulva lactuca* and its activated carbon, J Hazard Mater 148 (2007) 216–228, https://doi.org/10.1016/j.jhazmat.2007.01.146.
[28] S. Rezania, M. Ponraj, A. Talaiekhozani, S.E. Mohamad, M.F. Md Din, S.M. Taib, F. Sabbagh, F.M. Sairan, Perspectives of phytoremediation using water hyacinth for removal of heavy metals, organic and inorganic pollutants in wastewater, J Environ Manag 1 (2015) 125–133, https://doi.org/10.1016/j.jenvman.2015.08.018.
[29] S.S. Dhiman, X. Zhao, J. Li, D. Kim, V.C. Kalia, I.W. Kim, J.Y. Kim, J.K. Lee, Metal accumulation by sunflower (Helianthus annuus L.) and the efficacy of its biomass in enzymatic saccharification, PLoS One 12 (2017) 1–14, https://doi.org/10.1371/journal.pone.0175845.
[30] L. Kim, G.-A. Catrina, G. Cernica, M. Popescu, C.I. Covaliu, Removal of metals from aqueous solutions using sea buckthorn waste from dietary supplement technology, Sustainability 13 (2021) 1–16, https://doi.org/10.3390/su13031441.
[31] E. Da'na, Nano-silica modified with diamine for capturing azo dye from aqueous solutions, Molecules 27 (2022) 1–16, https://doi.org/10.3390/molecules27113366.
[32] J.M. Zhou, Z.C. Jiang, X.Q. Qin, L.K. Zhang, Q.B. Huang, G.L. Xu, D.D. Dionysiou, Efficiency of Pb, Zn, Cd, and Mn removal from karst water by Eichhornia crassipes, Int J Environ Res Publ Health 17 (2020) 1–15, https://doi.org/10.3390/ijerph17155329.
[33] V.N. Thekkudan, V.K. Vaidyanathan, S.K. Ponnusamy, C. Charles, S. Sundar, D. Vishnu, S. Anbalagan, V.K. Vaithyanathan, S. Subramanian, Review on nano-adsorbents: a solution for heavy metal removal from wastewater, IET Nanobiotechnol 11 (2017) 213–224, https://doi.org/10.1049/iet-nbt.2015.0114.
[34] G. Wang, J. Wang, X. Guo, Y. Chen, Efficient removal of humic acid in water using a novel TiO_2 composite with biochar doping, RSC Adv 12 (2022) 31966–31975, https://doi.org/10.1039/d2ra05358f.
[35] S.M. Alardhi, T.M. Albayati, J.M. Alrubaye, Adsorption of the methyl green dye pollutant from aqueous solution using mesoporous materials MCM-41 in a fixed-bed column, Heliyon 6 (2020) e03253, https://doi.org/10.1016/j.heliyon.2020.e03253.
[36] I.K. Abd ali, T.A. Ibrahim, A.D. Farhan, M.N. Abbas, Study of the effect of pesticide 2,4-D on the histological structure of the lungs in the albino mice (*Mus musculus*), J Pharmaceut Sci Res 10 (2018) 1418–1421.
[37] E.E. Chang, J.C. Wan, H. Kim, C.H. Liang, Y.D. Dai, P.C. Chiang, Adsorption of selected pharmaceutical compounds onto activated carbon in dilute aqueous solutions exemplified by acetaminophen, diclofenac, and sulfamethoxazole, Sci World J 186501 (2015) 1–11, https://doi.org/10.1155/2015/186501.
[38] X. Ren, H. Feng, M. Zhao, X. Zhou, X. Zhu, X. Ouyang, J. Tang, C. Li, J. Wang, W. Tang, L. Tang, Recent advances in thallium removal from water environment by metal oxide material, Int J Environ Res Public Health 20 (2023) 1–22, https://doi.org/10.3390/ijerph20053829.
[39] A.D.M.d. Medeiros, C.J.G.d. Silva Junior, J.D.P.d. Amorim, I.J.B. Durval, Oily wastewater treatment: methods, challenges, and trends, Processes 10 (2022) 1–20, https://doi.org/10.3390/pr10040743.
[40] Z. Wang, Z. Feng, L. Yang, M. Wang, Effective removal of calcium and magnesium ions from water by a novel alginate-citrate composite aerogel, Gels (Basel, Switzerland) 7 (2021) 1–13, https://doi.org/10.3390/gels7030125.
[41] K. Shen, L. Cui, L. Yang, X. Wei, X. Liu, M. Ren, F. Cao, J. Xu, Molecular dynamics simulations of the nickel removal from crude oil by neutral and charged spherical polymer brushes, Fuel 345 (2023) 1–9, https://doi.org/10.1016/j.fuel.2023.128179. Article No. 128179.
[42] H. Yu, C. Li, J. Yan, Y. Ma, X. Zhou, W. Yu, H. Kan, Q. Meng, R. Xie, P. Dong, A review on adsorption characteristics and influencing mechanism of heavy metals in farmland soil, RSC Adv 13 (2023) 3505–3519, https://doi.org/10.1039/d2ra07095b.
[43] M.N. Abbas, S.A. Ibrahim, Z.N. Abbas, T.A. Ibrahim, Eggshells as a sustainable source for acetone production, JKSUES 34 (2022) 381–387, https://doi.org/10.1016/j.jksues.2021.01.005.
[44] J.K. Saini, R. Saini, L. Tewari, Lignocellulosic agriculture wastes as biomass feedstocks for second-generation bioethanol production: concepts and recent developments, 3 Biotech 5 (2015) 337–353, https://doi.org/10.1007/s13205-014-0246-5.
[45] Ł. Wujcicki, J. Kluczka, Recovery of phosphate(V) ions from water and wastewater using chitosan-based sorbents modified-A literature review, Int J Mol Sci 24 (2023) 1–28, https://doi.org/10.3390/ijms241512060.
[46] T. Wu, H. Peng, X. Liu, R. Wu, Removal of carbamazepine in aqueous solution by CoS2/Fe^{2+}/PMS process, Molecules 27 (2022) 1–11, https://doi.org/10.3390/molecules27144524.
[47] A. Kumar, M. Nagar, Histomorphometric study of testis in deltamethrin treated albino rats, Toxicol Rep 1 (2014) 401–410, https://doi.org/10.1016/j.toxrep.2014.07.005.
[48] K. Moolchandani, A. Sharma, D. Kishan, Enhancing concrete performance with crumb rubber and waste materials: a study on mechanical and durability properties, Buildings 14 (2024) 1–22, https://doi.org/10.3390/buildings14010161.
[49] F.A.S. Hansted, D.Z. Mantegazini, T.M. Ribeiro, C.E.C. Gonçalves, J.A.P. Balestieri, A mini-review on the use of waste in the production of sustainable Portland cement composites, Waste Manag Res 41 (2023) 828–838, https://doi.org/10.1177/0734242X221135246.
[50] S.M. Abdelbasir, K.M. McCourt, D.C. Vanegas, Waste-Derived nanoparticles: synthesis approaches, environmental applications, and sustainability considerations, Front Chem 8 (2020) 1–18, https://doi.org/10.3389/fchem.2020.0078.
[51] B. Zhao, C. Wang, H. Bian, A "Wastes-Treat-Wastes" technology: role and potential of spent fluid catalytic cracking catalysts assisted pyrolysis of discarded car tires, Polymers 13 (2021) 1–14, https://doi.org/10.3390/polym13162732.

[52] D. Ramutshatsha-Makhwedzha, A. Mavhungu, M.L. Moropeng, R. Mbaya, Activated carbon derived from waste orange and lemon peels for the adsorption of methyl orange and methylene blue dyes from wastewater, Heliyon 8 (2022) e09930, https://doi.org/10.1016/j.heliyon.2022.e09930.
[53] Z. Maqbool, W. Khalid, H.T. Atiq, H. Koraqi, Z. Javaid, S.K. Alhag, L.A. Al-Shuraym, D.M.D. Bader, M. Almarzuq, M. Afifi, A. Al-Farga, Citrus waste as source of bioactive compounds: extraction and utilization in health and food industry, Molecules 28 (2023) 1–20, https://doi.org/10.3390/molecules28041636.
[54] X. Jaramillo-Fierro, J. Ramón, E. Valarezo, Cyanide removal by ZnTiO3/TiO2/H2O2/UVB system: a theoretical-experimental approach, Int J Mol Sci 24 (2023) 1–34, https://doi.org/10.3390/ijms242216446.
[55] Z. You, X. Li, J. Huang, R. Chen, J. Peng, W. Kong, F. Liu, Agarose film-based liquid-solid conversion for heavy metal detection of water samples by laser-induced breakdown spectroscopy, Molecules 28 (2023) 1–14, https://doi.org/10.3390/molecules28062777.
[56] A. El Jery, H.S.K. Alawamleh, M.H. Sami, A. Ahsan, M.A. Imteaz, A. Shanableh, M. Shafiquzzaman, H. Osman, N. Al-Ansari, Isotherms, kinetics and thermodynamic mechanism of methylene blue dye adsorption on synthesized activated carbon, Sci Rep 14 (2024) 1–12, https://doi.org/10.1038/s41598-023-50937-0.
[57] E. Šabanović, M. Memić, J. Sulejmanović, A. Selović, Simultaneous adsorption of heavy metals from water by novel lemon-peel based biomaterial, Pol J Chem Technol 22 (2020) 46–53, https://doi.org/10.2478/pjct-2020-0007.
[58] M. Villen-Guzman, M.M. Cerrillo-Gonzalez, J.M. Paz-Garcia, J.M. Rodriguez-Maroto, B. Arhoun, Valorization of lemon peel waste as biosorbent for the simultaneous removal of nickel and cadmium from industrial effluents, Environ Technol Innov 21 (2021) 1–11, https://doi.org/10.1016/j.eti.2021.101380. Article No. 101380.
[59] S.H. Hasan, D. Ranjan, Agro-industrial waste: a low-cost option for the biosorptive remediation of selenium anions, Ind Eng Chem Res 49 (2010) 8927–8934, https://doi.org/10.1021/ie100622c.